(20) Unpublished results. The NMR study and the photochemical reactions of the unsymmetrically N,N-disubstituted α-oxoamides in solution will be published elsewhere. For NMR study on unsymmetrically N-substituted amides using lanthanide shift reagents, see A. H. Lewin and R. Alekel, *J. Am. Chem. Soc.*, **98**, 6919 (1976), and references cited therein.
(21) Under the following conditions, the lanthanide induced shift in the methyl group of the major isomer was 140 Hz, while that of the minor isomer was 28 Hz (0.4 M **1f** + 0.08 M Eu(fod)$_3$ in $CDCl_3$; 60 MHz; Eu(fod)$_3$, tris(heptafluorobutanoylpivaloylmethanato)europium.
(22) W. E. Stewart and T. H. Siddall, III, *Chem. Rev.*, **70**, 517 (1970); Y. Shvo, E. C. Taylor, K. Mislow, and M. Raban, *J. Am. Chem. Soc.*, **89**, 4910 (1967).
(23) In most unsymmetrically N-substituted amides, the configuration about the C–N bond in the crystalline state is same as that of the predominant isomer in solution; B. F. Pedersen and B. Pedersen, *Tetrahedron Lett.*, 2995 (1965); C. J. Brown and D. E. C. Cordridge, *Acta Crystallogr.*, 7, 711 (1954); A. H. Lewin, M. Frucht, K. V. J. Chen, E. Benedetti, and B. DiBlasio, *Tetrahedron*, **31**, 207 (1975).
(24) P. J. Wagner, I. E. Kochevar, and A. E. Kemppainen, *J. Am. Chem. Soc.* **94**, 7489 (1972).
(25) S. L. Shapiro, I. M. Rose, F. C. Testa, E. Roskin, and L. Freedman, *J. Am. Chem. Soc.*, **81**, 6498 (1959).

Chemiluminescent Reactions of Lucigenin. 1. Reactions of Lucigenin with Hydrogen Peroxide

Richard Maskiewicz, Dotsevi Sogah, and Thomas C. Bruice*

Contribution from the Department of Chemistry, University of California at Santa Barbara, Santa Barbara, California 93106. *Received December 26, 1978*

Abstract: The chemiluminescent reaction of lucigenin (*N,N'*-dimethyl-9,9'-biacridine, **1**) at various pH values (solvent H_2O, 30 °C, μ = 1.0) with hydrogen peroxide in excess is first order to 6 half-lives. At constant pH the reaction rate was determined to be dependent upon the first power of the concentration of hydrogen peroxide and to be independent of concentrations of **1** and buffers. From the pH dependence of the pseudo-first-order rate constant (k_{obsd}, $[H_2O_2]_T \gg [\mathbf{1}]$) the rate of disappearance of **1** follows the general expression $d[\mathbf{1}]/dt = [\mathbf{1}]\{k_1[HO_2^-] + k_2[HO_2^-][HO^-]\}$. Diminution in light emission with time was shown to follow the same rate law and the quantum yield was established to be independent of [**1**], total hydrogen peroxide concentration ($[H_2O_2]_T$), and pH. These results establish that the chemiluminescent reaction of **1** with hydrogen peroxide follows the same rate law as does the overall disappearance of **1** from solution in the presence of varying concentrations of H_2O_2 and at all pH values. Replacement of H_2O with t-BuO_2H provides less light than obtained in the absence of any peroxide agent. Lucigenin reacts with H_2O_2 and t-BuO_2H at various pH values to produce *N*-methylacridone (**2**) as the major fluorescent product. The chemiluminescent spectrum at any time could be shown to result from emission by excited **2** and subsequent absorption by **1**. Competing dioxetane and linear peroxide mechanisms (with H_2O_2 and t-BuO_2H) are proposed and discussed. Evidence is presented which suggests that the 9,9'-dioxetane of **1** provides **2** + **2*** by the two competing pathways of spontaneous fragmentation and $1e^-$ transfer.

Introduction

Lophine (1877),[1] luminol (1928),[2] and lucigenin (1935)[3] stand as the classic organic chemiluminescent agents. Of these three compounds, the chemiluminescent (CL) reactions of *N,N'*-dimethyl-9,9'-biacridine (lucigenin, **1**) are possibly the least understood. Indeed, chemiluminescence has been reported to occur on the addition of numerous nucleophiles and reducing agents to solutions of **1**. However, none of these studies included a systematic approach to the mechanism of the CL reactions; few workers have even bothered to maintain constant pH. The application of kinetic methods to the elucidation of the mechanism of CL reactions may, by itself, be of limited use for the simple reason that light production may represent a minor reaction path. However, it is well appreciated[4] that the rate laws for both of two parallel reactions may be determined from the overall kinetic expression for disappearance of the common substrate and the fractional yield of product arising from the minor reaction. Light is a product of the minor CL reaction and the chemiluminescent quantum yield (Φ_{CL}) is a measure of the fractional yield of the minor reaction. As a pertinent example, consider the reactions of eq I where the

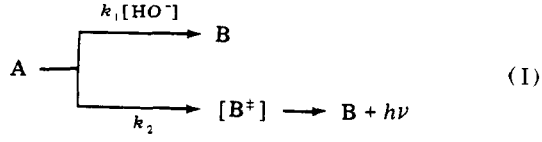

(I)

major reaction is not light producing. At constant pH the rate of disappearance of A and appearance of B will be pseudo first order and the pseudo-first-order rate constant (k_ψ) will be equal to $k_1[HO^-] + k_2$. Since $k_1[HO^-] \gg k_2$, $k_\psi = k_1[HO^-]$, so that the rates of disappearance of A and (appearance of B) will be under the kinetic control of the major reaction path. For this reason a plot of log k_ψ vs. pH will be of slope +1. A plot of the logarithm of the first-order rate constants for decay of photon emission vs. pH will necessarily also be linear and of slope +1. If α is defined as the mole fraction of A that passes through the CL pathway (i.e., $\alpha = k_2/k_1[HO^-]$), then α is equivalent to Φ_{ex}, the overall efficiency of producing the excited state $B^{\ddagger}$, and directly proportional to the quantum yield (Φ_{CL}). It follows from eq I that a plot of log Φ_{CL} ($= \Phi_{fl}k_2/k_1[HO^-]$ where Φ_{fl} is the fluorescence quantum yield equating Φ_{fl} to α) vs. pH would be linear but of slope −1. Such a relationship would establish that the very minor CL reaction is independent of $[HO^-]$. If both the major reaction and the minor CL reaction were of the same order in HO^-, H_3O^+, X, etc., then a change in the concentrations of these reagents would not alter Φ_{CL}. This approach has been employed herein to establish the composition of the transition state for the CL reaction of **1** with hydrogen peroxide.

Experimental Section

Materials. *N,N'*-Dimethyl-9,9'-biacridinium nitrate (1) (Aldrich Chemical Co.) was repeatedly recrystallized from ethanol–water (5/95 v/v) to give orange crystals that were dried at 100 °C (0.1 mmHg) for 24 h, mp 250 °C dec (lit.[5] 250 °C). UV-vis (water, pH 3.72): 453 nm (log ϵ 3.93), 430 (4.03), 420 (3.95), 369 (4.55), 354 (4.24), 260 (5.22). *N*-Methylacridone (**2**) was prepared by a literature procedure[6] and recrystallized (three times) from absolute ethanol to give yellow crystals (needles) that melted at 210–211 °C (lit.[6] 209–210

0002-7863/79/1501-5347$01.00/0

°C). Anal. Calcd for $C_{14}H_{11}OH$: C, 80.38; H, 5.26; N, 6.70. Found: C, 80.34; H, 5.30; N, 6.60.

Reagents and solvents including hydrogen peroxide (stabilized, 30%) were all analytical or spectroscopic grade and used as obtained. *tert*-Butyl hydroperoxide was purified six times by precipitation from strong base.[7] Deionized and doubly distilled water was employed for the preparation of all kinetic solutions. Trace metals were removed from selected solutions with Chelex-100 cation exchange resin.

Apparatus. Ultraviolet and visible spectra and absorbance measurements were recorded on Cary 15, 16, or 118 spectrophotometers. Measurements of pH were performed with a Radiometer Model 26 pH meter equipped with Model EA-125 (Metrohm) or GK-2302C (Radiometer) electrodes. High-pressure liquid chromatographic analyses were carried out on a Lichrosorb reverse phase (10 × 250 nm, 10-μ particles) column using a Schoeffel Instrument SF 770 spectroflow monitor equipped with an Altex solvent metering system Model 100 and a Varian Associates CDC 101 integrater. Photon counting was carried out with quantum photometers Model 1140A (Princeton Applied Research) equipped with 1P28A photomultiplier tubes (30 °C). Fluorescence measurements were performed with either a Perkin-Elmer Model 512 double beam fluorescence spectrophotometer or a Perkin-Elmer Model MPF-3 fluorescence spectrophotometer thermostated at 30 °C. Analyses of all data were performed with the aid of either an iterative reaction kinetics simulator PDP 11/03 (Tektronic) or a Hewlett-Packard calculator, Model 9862A plotter. Melting points were taken with a Thomas-Hoover capillary melting point apparatus and are uncorrected. Polarographic studies were carried out on a modified Princeton Applied Research Model 174 polarographic analyzer. Solutions were deoxygenated by passing a stream of N_2 through them for 0.5 h. Half-wave potentials were measured in aqueous solutions relative to a saturated calomel electrode at 25 °C with a dropping mercury electrode.

Methods. Reaction with Hydrogen Peroxide. Spectrophotometric runs were performed on 3.10 mL of reaction mixture (containing Na_2EDTA (10^{-4} M), H_2O_2 at desired concentration, and lucigenin (3.66×10^{-6} M)) using a Gilford spectrophotometer at 369 nm. Hydrogen peroxide was added to the buffer before the final pH adjustment. Phosphate (pH 7-9; 11.3-13.3), carbonate (pH 9-11.3), and KOH (pH >13.3) were used as buffers. Reactions were also performed using the reactants H_2O_2 and *t*-BuOOH as buffers in the pH range of $pK_a \pm 1$. Measurements of CL emission were performed on 5.05 mL of the reaction solutions (Na_2EDTA = ca. 10^{-4} M, [**1**] = 1.12×10^{-7} M, and $[H_2O_2]$ at the desired concentration). Kinetic runs were performed in both the presence and absence of KCl to maintain μ = 1 and in the absence of Na_2EDTA in cases where trace metals were removed via a cation exchange resin.

Reaction with *tert*-Butyl Hydroperoxide. Chemiluminescence emission measurements were carried out on a total volume of 4.50 mL (Na_2EDTA (ca. 10^{-4} M), lucigenin (1.8×10^{-5} M) and *t*-BuOOH (0.01-0.15 M)). Potassium hydroxide was used to adjust basicity at all pH values. Hydrogen peroxide solutions were standardized with potassium permanganate while the exact concentration of *tert*-butyl hydroperoxide was determined by sample weight.

Product Analysis of the Chemiluminescence Reaction of Lucigenin with Hydrogen Peroxide. A. Analytical Scale. High-pressure liquid chromatographic (LC) analysis was performed on the kinetic runs at pH 10.50, 11.60, 12.25, and 13.42. Typically, 100 mL of lucigenin solution (1.02×10^{-3} M) was mixed with 6.0 mL of desired buffer (H_2O_2, 0.049 M; Na_2EDTA, 9.9×10^{-5} M). After light emission had ceased the reaction mixture was extracted with 2.0 mL of chloroform (spectroscopic grade). The chloroform was evaporated to dryness by bubbling a stream of nitrogen through it. The dry residue was dissolved in 0.50 mL of 30/70 (v/v) 2-propanol/water and an aliquot of the solution (100 μL) was then introduced onto the LC column (Lichrosorb 10 × 250 mm reversed phase) and eluted with the same solvent mixture. With the detector wavelength at 255 nm and a flow rate of 2.0 mL/min, one peak was recorded with retention time of 40.80 min. This peak was identified to be *N*-methylacridone by comparing the retention time of the latter with that of the unknown under identical conditions. *N*-Methylacridone has a retention time of 40.90 min. Injection of 100 μL of the aqueous layer onto the same column followed by elution with the same solvent system gave three compounds with retention times of 8.32, 9.63, and 10.43 min.

B. Large-Scale Product Analysis. Lucigenin (233 mg, 0.45 mmol) was dissolved in 15 mL of distilled water in a 250-mL conical flask. To this were added 100 mL of phosphate buffer (pH 11.60) containing 15 mL of 30% hydrogen peroxide and 5 mL of 0.10 M Na_2EDTA in the dark. The flask, wrapped in aluminum foil, was allowed to stand in the dark (with occasional shaking) for a total of 24 h, after which 50 mL of $CHCl_3$ was added. The two layers were thoroughly mixed and then allowed to separate. The organic layer was removed and the aqueous layer extracted thrice with $CHCl_3$ (3 × 50 mL). The washings were combined, dried over $MgSO_4$, filtered, and then evaporated to dryness in vacuo to leave a yellowish solid that weighed 181 mg. This was recrystallized once from absolute ethanol to give an unidentified material (yellow needles) that melted at 250 °C and weighed 51 mg. Concentrating the mother liquor to about 5 mL and allowing it to stand at 4 °C yielded *N*-methylacridone, 124 mg (mp 210-211 °C). The NMR, UV, and IR spectra were identical with those of authentic **2**. The other product was nonfluorescent and its NMR showed peaks at δ 3.89, singlet, 3 H (NCH_3); 4.08, 3 H (NCH_3); 6.13-6.74, multiplet, 4 H; 7.26-7.48, multiplet, 4 H; 7.55-7.78, multiplet, 3 H; 7.81-7.87, doublet, 3 H; 7.90-8.00, multiplet, 3 H. The UV spectrum shows peaks at λ_{max} 330 and 277 nm.

Applying the same procedure to runs at pH 10.50, 12.50, and 13.50, *N*-methylacridone was isolated in 70, 80, and 85% yields, respectively, while only traces of the minor product obtained at pH 11.60 were obtained at pH 12.50 and 13.50. At pH 10.50 the yield of the nonfluorescent product was the same as that obtained at pH 11.60.

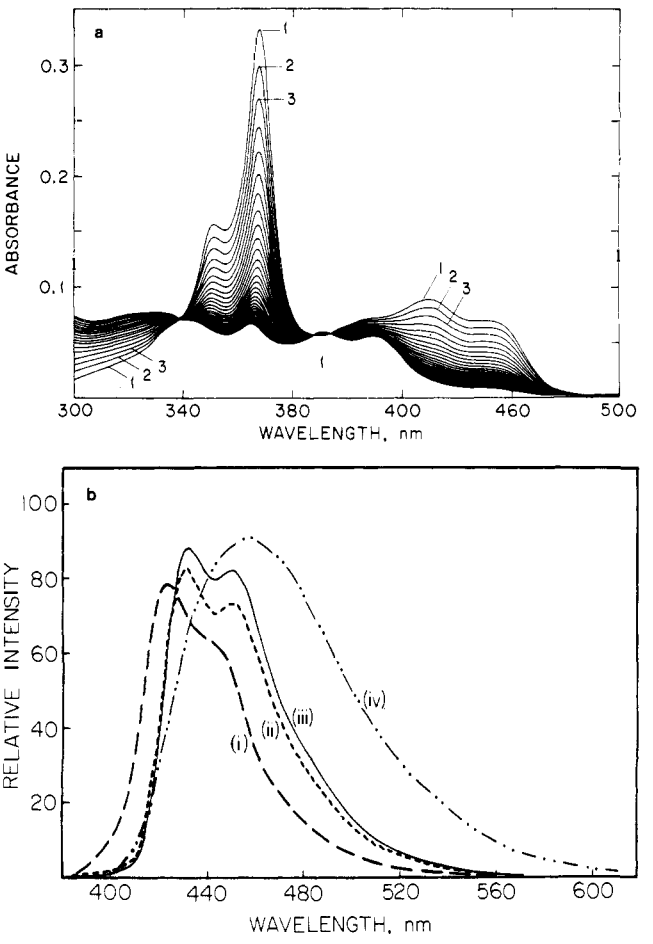

Figure 1. (a) Repetitive spectral scans of the time course for the reaction of **1** with basic hydrogen peroxide at pH 11.26. The time interval between any two consecutive scans is 136 s. Lucigenin concentration, 9.46×10^{-6} M; hydrogen peroxide, 9.79×10^{-2} M. (b) Fluorescence emission spectrum of *N*-methylacridone in ethanol (curve i) at pH 13 (curve ii); fluoresence emission (curve iii) and chemiluminescence (curve iv) spectra of the reaction with H_2O_2 at pH 13.

Results

The rates of disappearance of **1** from solution (solvent H_2O, 30 °C, μ = 1.0) were followed spectrophotometrically. Figure 1a represents a typical repetitive scan of the time course of the reaction. Inspection of Figure 1a reveals that the disappearance

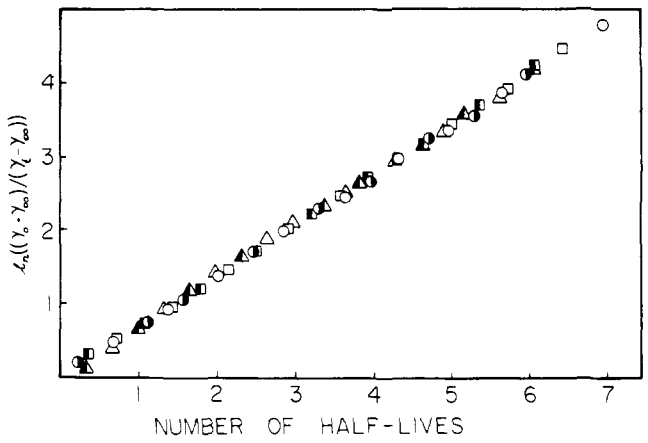

Figure 2. Plots of $\ln((\gamma_0 - \gamma_\infty)/\gamma_t - \gamma_\infty))$ vs. half-lives for reaction of **1** with hydrogen peroxide at pH 10 (△, CL emission; ▲, spectrophotometric), 12.18 (□, CL emission; ■, spectrophotometric), and 13.18 (○, CL emission; ●, spectrophotometric). γ_0 = initial absorbance or intensity; γ_∞ = final absorbance or intensity; γ_t = absorbance or intensity at time t.

Table I. Rate Constants Employed to Fit Equation 1 to the Experimental Log k_{obsd} vs. pH Profiles for Lucigenin Disappearance and to the Log k_b vs. pH Plot for the Decay of Quanta Emission (Solvent H_2O; 30 °C; $[H_2O_2]_T$ = 0.035 M)

	$A_{369}(k_{obsd})$	$h\nu(k_b)$
k_1, $M^{-1}\,s^{-1}$	3.5×10^{-3}	4.2×10^{-3}
k_2, $M^{-2}\,s^{-1}$	9.0×10^{-4}	2.9×10^{-3}
pK_{app}	11.30	11.30

Table II. Slopes and Intercepts for the Plots of k_b vs. $[H_2O_2]_T$

pH	slope, $M^{-1}\,s^{-1}$	intercept, s^{-1}
10.74	3.43×10^{-3}	very small
11.32	7.73×10^{-3}	$\sim 10^{-6}$
12.42	2.68×10^{-2}	1.96×10^{-5}
13.54	3.51×10^{-2}	2.86×10^{-4}

of **1** is accompanied by isosbestic points at 339, 388, 394, and 482 nm. This feature speaks against the accumulation of any intermediate differing significantly in its spectrum from **1**. However, since the pseudobase of **1** possesses an extinction coefficient differing very little from that of **1**,[8] some appreciable concentration of an adduct of HO_2^- and **1** may well escape spectral detection. In practice the disappearance of **1** was followed at 369 nm and the decrease in A_{369} was found to follow the first-order rate law to 6 half-lives (Figure 2) between pH 9.50 and 14.0 and to at least 3 half-lives between pH 8 and 9.50. A plot of the logarithm of the pseudo-first-order rate constants for disappearance of **1** vs. the pH of the rate determination is provided in Figure 3a. The circular points of the figure are experimental and the best line connecting the points is generated from the equation

$$k_{obsd} = \left\{\frac{k_1 K_{H_2O_2}}{K_{H_2O_2} + a_H} + \frac{k_2 K_{H_2O_2} K_w}{a_H(K_{H_2O_2} + a_H)}\right\}[H_2O_2] \quad (1)$$

or

$$k_{obsd} = k_1[HO_2^-] + k_2[HO_2^-][HO^-] \quad (1a)$$

(employing the numerical rate constants of Table I), where K_w is the autoprotolysis constant of water (13.833[9]), a_H is the hydrogen ion activity as determined by glass electrode, and $K_{H_2O_2}$ is the acid dissociation constant for hydrogen peroxide. The value of $pK_{H_2O_2}$ = 11.62[10] may be compared to the kinetic

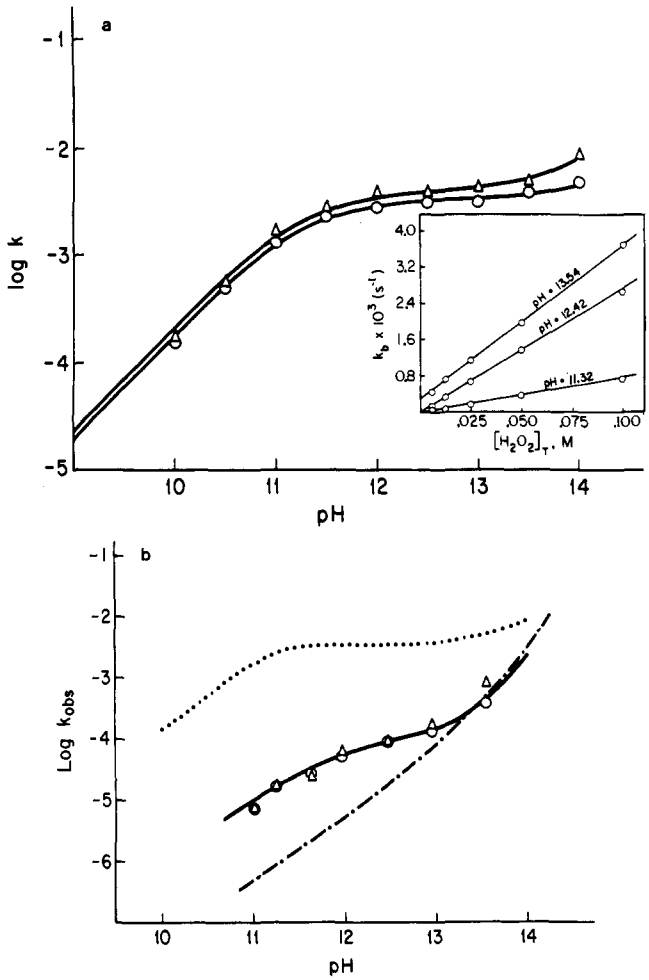

Figure 3. (a) pH-log (rate) profiles for reaction of lucigenin with basic hydrogen peroxide from spectrophotometric rates (○), and rates of decay of light emission (△). Initial concentrations: H_2O_2, 0.049 M; lucigenin, 1.12×10^{-7} (pH 9.50–14) and 1.061×10^{-5} M (pH 8–9); Na_2EDTA, 10^{-4} M. Inset: plots of k_b (rates of light decay) vs. total concentration of hydrogen peroxide at pH 11.32, 12.42, and 13.54 and lucigenin concentration of 1.12×10^{-7} M. (b) pH vs. log rate profiles (light decay) for reaction of lucigenin with t-BuO_2H (○), hydroxide[8] (- - -), and hydrogen peroxide (·····).

pK_{app} (Table I) value employed for the computation of the log k_{obsd} vs. pH profile.

In the determination of the *kinetics for light emission* the photon counting data were collected as plots of photons emitted per second (cps) vs. time. The decay of light emission (k_b) followed the first-order rate law. The log k_b vs. pH profile, determined at $[H_2O_2]_T$ = 0.035 M, is shown in Figure 3a as triangular points. The line connecting the points is generated from eq 1 (with k_b replacing k_{obsd}) employing the appropriate constants from Table I. Comparison of the pH-rate profiles for the disappearance of **1** (k_{obsd}) and decay of light emission (k_b) reveals that the values of k_{obsd} and k_b are about the same between pH 8 and 12.68 (k_1 constants of Table I). Above pH 12.7 the values of k_b become greater than k_{obsd} (compare k_2 values of Table I).

In the pH range 8–13 the rate of disappearance of **1** and decay of light were first order in $[H_2O_2]_T$. ($[H_2O_2]_T$ was varied between 6×10^{-3} and 1×10^{-1} M. At $[H_2O_2]_T \gg 0.1$ M, oxygen bubble formation precluded kinetic determinations, particularly at high base concentrations.) Plots of k_b vs. $[H_2O_2]_T$ at pH 11.32, 12.42, and 13.54 are found to be linear and are shown in Figure 3a (inset), while the slopes and the intercepts of the lines are recorded in Table II. The intercepts of the peroxide dilution plots at $[H_2O_2]_T$ = 0 correspond to the

Table III. Pseudo-First-Order Rate Constants for Disappearance of Lucigenin (A_{369}) as a Function of Buffer Concentration ($[H_2O_2]_T$ = 0.048 M; [Lucigenin] = 9.56×10^{-6} M; Carbonate Buffer; 30 °C)

	k_{obsd}, s^{-1}	
$[buffer]_T$, M	pH 9.50	pH 10.71
0.05	1.61×10^{-5}	2.08×10^{-4}
0.10	2.00×10^{-5}	2.23×10^{-4}
0.25	2.10×10^{-5}	2.20×10^{-4}
0.50	2.00×10^{-5}	2.22×10^{-4}

Table IV. Percentage Yields of *N*-Methylacridone and "Trapped" Lucigenin Determined by LC Analysis (2) and Manual Workup (3)

	method (2)		method (3)	
pH	**2**	**1**	**2**	**1**
10.50	52	18	70	0
11.60	51	17	63	0
12.25	57	15	80	0
13.43	83	5	85	0

pseudo-first-order rate constants in the absence of H_2O_2 (i.e., HO^--catalyzed aerobic oxidation).[8] At pH 13.92 (μ = 1) the value of $k_{obsd} = 2.35 \times 10^{-3}$ s^{-1} for the disappearance of **1** in the absence of H_2O_2 approaches $k_{obsd} = 4.13 \times 10^{-3}$ s^{-1} obtained in the presence of 0.049 M H_2O_2. At $[OH^-] > 1$ M the values of k_{obsd} in the presence and absence of H_2O_2 appear identical. The mechanism of the CL reaction of HO^- with **1** in the presence of O_2 is the subject of the following paper.[8]

The pseudo-first-order rate constants for both disappearance of lucigenin and decay of CL emission were found to be buffer independent. Thus, as shown in Table III, a tenfold variation in buffer concentration produces no appreciable change in the observed rate constants for disappearance of lucigenin (A_{369}) at pH 9.50 and 10.71. In phosphate buffer (0.10 M) at pH 11.58, 12.43, and 13.42 the observed rate constants for decay of CL emission are 8.19×10^{-4}, 1.58×10^{-3}, and 7.93×10^{-3} s^{-1}, respectively, while in the absence of buffer other than KOH the rate constants were determined to be 7.95×10^{-4}, 1.55×10^{-3}, and 6.73×10^{-3} s^{-1}, respectively ($[H_2O_2]_T$ = 0.048 M, **1** = 1.12×10^{-7} M). These results suggest that only specific base catalysis occurs.

Product analyses were carried out by (1) fluorescence spectroscopy of reaction mixtures; (2) LC analysis of the kinetic runs immediately following completion of light production; (3) manual workup of preparative-scale reactions at some considerable period of time following completion of reaction (ca. 18-24 h). The emission spectrum of products at the end of the CL reaction at pH 13 (Figure 1b) is accounted for by the emission spectrum of *N*-methylacridone (**2**). Analysis by procedure (2) indicates that at the completion of the CL reaction there is present in solution, **2**, a compound analyzing as unreacted **1** and small concentrations of two unidentified compounds (see Table IV). At the time of isolation by method (3) all of **1** has disappeared from solution. Although a direct comparison between methods (2) and (3) is not possible because of large differences in initial concentrations, it appears that the formation of **2** from a compound analyzing as **1** continues after cessation of light production. Accompanying the continued formation of **2** there arises a nonfluorescent material (51 mg from 233 mg of **1** below ~pH 12 and traces above pH 12) absorbing at 330 and 277 nm.

The isolation of **1** at a time when the CL reaction has gone to completion suggests the possibilities that (a) H_2O_2, though used in excess over **1**, has been depleted; (b) a quencher is formed from **1** by first-order kinetics so that the resultant first-order rate of decrease of quantum emission is increased relative to that for disappearance of **1**; (c) **1** is converted, in a side reaction, to a compound which possesses a spectrum similar to **1** and which readily reconverts to **1** on change of solvent, pH, etc. That the $[H_2O_2]_T$ does not change appreciably during the course of the CL reaction was shown by the following experiments. At completion of the CL reaction (pH 13) the addition of an aliquot of a concentrated solution of **1** reinitiates light production. Further, if the concentration of **1** was brought to that value employed to initiate the first CL reaction, then it could be shown that the ensuing exponential decay of light production possessed the same rate constant as that for the initial reaction and most importantly the same Φ_{CL}. In short the decrease in $[H_2O_2]_T$ is imperceptible and any **1** remaining at completion of reaction must be in a form which does not enter CL reactions with H_2O_2. If at completion of the CL reaction there is added an aliquot of H_2O_2 (sufficient to double its initial concentration) the ensuing CL reaction amounts to only 1-3% of the quantum yield obtained initially. Formation of a quencher is precluded on the basis that deviation of the values of k_{obsd} and k_b increases with pH whereas the value of Φ remains constant. That **1** is partially converted to an inactive derivative was then shown by experiments in which the reaction solution, at completion of chemiluminescence, was acidified (to pH ~2) and then readjusted to pH 13. The ensuing CL reaction possessed a Φ equal to 5-10% of the original reaction in agreement with expectations from Table IV. Possible structures for the CL inert form of **1** include the dipseudobase (**3**) and epoxide (**4**). Both **3** and **4** possess spectra quite similar to that of **1**.[8]

Table V. Dependence of Quantum Yield upon $[H_2O_2]$ at Constant pH

$[H_2O_2]$, M	pH 11.32	pH 12.43
0.006	*a*	1.1×10^{-2}
0.0125	9.0×10^{-3}	*a*
0.025	7.2×10^{-3}	1.1×10^{-2}
0.050	1.0×10^{-2}	9.7×10^{-3}
0.100	8.3×10^{-3}	9.1×10^{-3}
av Φ_{obsd}	8.7×10^{-3}	1.0×10^{-2}

[a] Not determined.

Table VI. Quantum Yield as a Function of pH ($[H_2O_2]_T$ = 0.035 M; 30 °C)

pH	Φ	pH	Φ
9.0	3.8×10^{-3}	12.95	1.3×10^{-2}
9.97	5.6×10^{-3}	14.00	1.3×10^{-2}
11.00	1.0×10^{-2}	14.60	1.4×10^{-2}
12.00	1.3×10^{-2}		

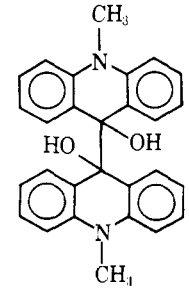

3

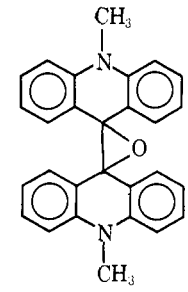

4

Chemiluminescence quantum yields (Φ_{CL}) were calculated from the area defined by the plots of cps vs. time. The values of Φ_{CL} were found to remain constant with increase in $[H_2O_2]_T$ at constant pH (Table V) and to be completely independent of pH above pH ~11, at constant $[H_2O_2]_T$ (Table VI). Also, both Φ_{CL} and rate constant (k_b) for decay of light emission are

Table VII. Quantum Yield (Φ_{CL}) and Rate Constant for Chemiluminescent Decay (k_b) as a Function of Lucigenin Concentration at Constant pH and $[H_2O_2]$ (pH 13.8, $[H_2O_2]$ = 0.045 M)

[1], M	Φ	k_b, s^{-1}
5.8×10^{-5}	11.3×10^{-3}	4.8×10^{-3}
3.5×10^{-6}	7.8×10^{-3}	5.0×10^{-3}
2.8×10^{-7}	8.8×10^{-3}	6.8×10^{-3}
1.4×10^{-7}	10.4×10^{-3}	7.4×10^{-3}
3.5×10^{-8}	8.5×10^{-3}	6.6×10^{-3}
8.8×10^{-9}	6.1×10^{-3}	7.9×10^{-3}
2.2×10^{-9}	12.5×10^{-3}	6.7×10^{-3}

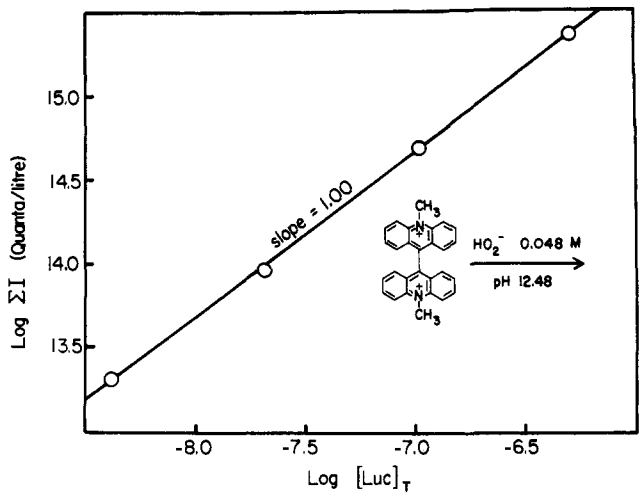

Figure 4. Total quanta emitted in the reaction of lucigenin and H_2O_2 as a function of [1].

independent of [1] at constant $[H_2O_2]_T$ and pH (Table VII). Hence, the plot of total quanta emitted per liter vs. concentration of lucigenin (Figure 4) is linear with a slope of 1.0.

Reaction of lucigenin with *tert*-butyl hydroperoxide was found to be weakly chemiluminescent. The intensity of the CL emission increases with time followed by exponential decay. The intensity vs. time plots (not shown) follow consecutive first-order kinetics

$$A \xrightarrow{k_a} B \xrightarrow{k_b} C + h\nu \qquad (2)$$

and were fitted by analogue simulation to the scheme of eq 2 in order to solve for the constant k_b. A plot of log k_b vs. pH (Figure 3b) resembles that for the reaction with hydrogen peroxide (Figure 3a). The first-order rate constant, k_b, for the decay of the CL emission obeys the rate law

$$k_{obsd} = \left(\frac{k_1 K_{a_1}}{K_{a_1} + a_H} + \frac{k_2 K_w}{a_H}\right)[t\text{-BuOOH}]_T + k_3\left(\frac{K_w}{a_H}\right)^2 \qquad (3)$$

The values of the various rate constants employed to fit the line to the experimental points are $k_1 = 1.08 \times 10^{-4}$ M^{-1} s^{-1}, $k_2 = 2.60 \times 10^{-4}$ M^{-1} s^{-1}, and $k_3 = 5.0 \times 10^{-3}$ M^{-2} s^{-1} with [*t*-BuOOH] = 0.035 M. The value of pK_{a_1} used to fit the curve is 11.9, which is lower than the acid dissociation constant for *tert*-butyl hydroperoxide ($pK_{t\text{-BuOOH}} = 12.8$[11]). The values of Φ in the reaction of *tert*-butyl hydroperoxide with **1** (Figure 5) exhibit the same pH independence as does the reaction of **1** with hydroxide ion.[8] The quantum yields for the aerobic *t*-BuO_2H reactions are, however, smaller than in the case of the aerobic hydroxide reaction.

Fluorescence and Chemiluminescent Spectra. Although the fluorescence spectra of the spent reaction mixtures (pH 8–14), when normalized, are exactly superimposable on that of *N*-methylacridone (**2**), the CL spectra are not. Figure 1b shows the fluorescence spectra of **2** in ethanol (i) and aqueous 0.10 M KOH (ii), the fluorescence spectrum of the spent reaction (iii), and the CL spectrum of the reaction of **1** with H_2O_2 in 0.10 M KOH (iv). Examination of Figure 1b leads to the following conclusions: (a) **2** represents the only major product of the reaction that possesses appreciable fluoresence; (b) if **2** is the primary emitting species then its energy is being transferred to a compound which fluoresces at longer wavelengths, or its emission spectrum is being modified to give the observed CL spectrum. In Figures 6a–c are provided the CL spectra at pH

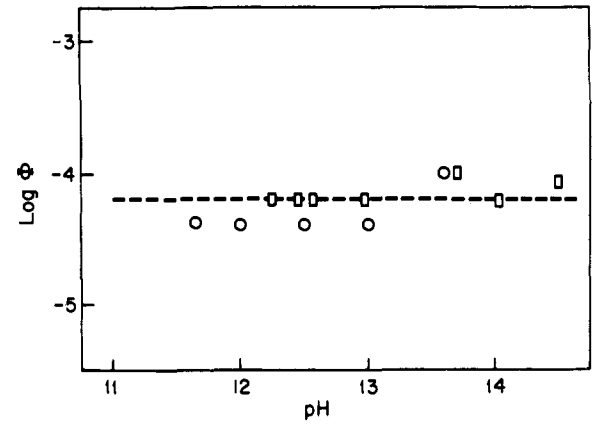

Figure 5. Quantum yields for reactions of **1** with *t*-BuO_2H (O) and hydroxide[8] (- - - -).

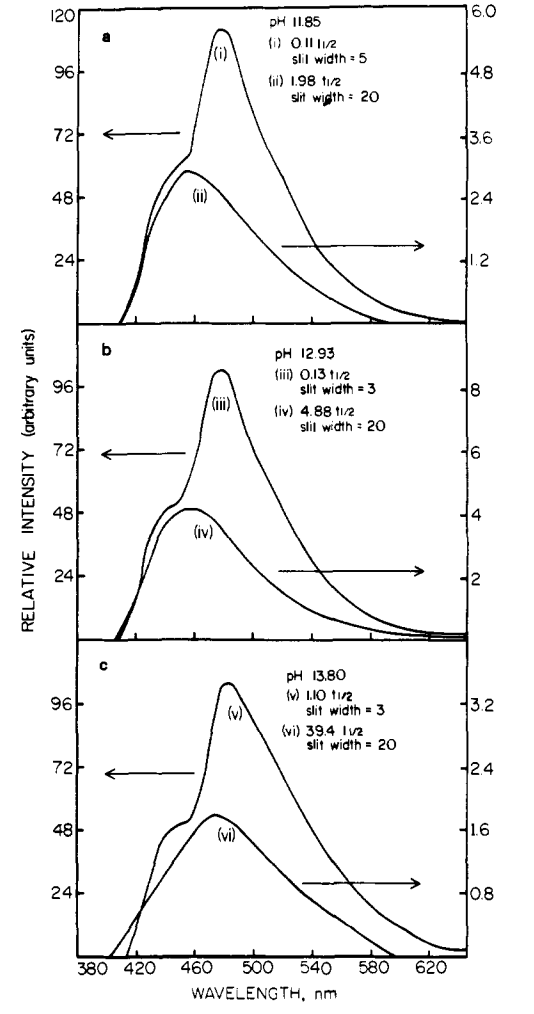

Figure 6. Change in observed chemiluminescence spectrum with time, at various pHs.

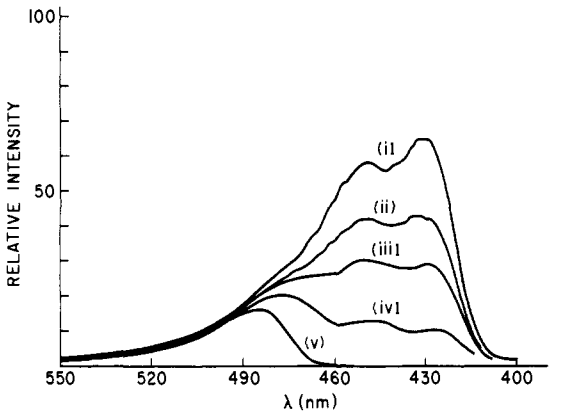

Figure 7. Effect of lucigenin solutions of varying concentrations (i, [1] = 0.0 M; ii, [1] = 2×10^{-5} M; iii, [1] = 4×10^{-5} M; iv, [1] = 6.6×10^{-5} M; v, [1] = 2×10^{-4} M) upon the emission spectrum of **2**, where the emission is passed through the above solutions.

values of 11.15 (curves i and ii), 12.93 (iii and iv), and 13.80 (v and vi), all recorded as a function of time. Figure 7 shows the effect of solutions of **1**, at various concentrations, on the emission spectrum of **2**, where the solutions of **1** were placed in a separate cuvette in the path between the irradiated acridone solution and the detector monochromator. The similarity between the CL spectra recorded immediately after mixing reactants (i, iii, and v of Figure 6) and the emission spectrum of **2** after passing through a concentrated solution of **1** (curve v of Figure 7) suggests that the observed CL spectrum results from absorption of **2*** emission by **1**. The corresponding similarity between curves ii, iv, and vi of Figure 6 (where **1** has been greatly depleted) and curves ii and iii of Figure 7, where [**1**] are low, supports this conclusion. Since the extent of absorption is dependent upon [**1**] it follows that as the CL reaction approaches completion its emission spectrum should approach the fluorescence spectrum of **2**. No evidence of energy transfer from **2*** → **1** or to compounds such as **3** and **4** was detected since emission spectra of combined solutions of **1** and **2** at both high and low pH values and at various [**1**] are strictly additive. That is, no additional increase in intensity of the emission spectrum of **1** was realized upon excitation of **2** in a solution of **1** plus **2**.

Discussion

The emitting species must be known as a preliminary to the understanding of the mechanism of any CL reaction. The results of Table IV established that the major product of the reaction of **1** and hydrogen peroxide at basic pHs is **2**. Furthermore, **2** is the only major fluorescent species present at completion of reactions (Figure 1b). That the primary emitter is singlet *N*-methylacridone (**2***) is not, however, immediately apparent from the CL spectrum, which is quite different from the emission spectrum of **2** (Figure 1b). No evidence for energy transfer from **2*** to **1** was detected when the observed emission spectra of mixtures **1** and **2** were compared to the sum of the emission spectra obtained from separate solutions of **1** and **2**. The observed CL spectrum can, however, be simulated by exciting acridone and passing its emission through solutions containing various concentrations of **1** (Figure 7). Therefore, the CL spectra result from absorption of emitted light from **2*** by **1** with **2*** being the primary emitter.

Elucidation of a reasonable mechanism for a minor CL reaction in competition with major non-light-producing reactions is possible by kinetic methods, if rate constants for starting material conversion and light decay are compared to quantum yields measured at the same reactant concentrations at which the rate constants were determined (see Introduction). The pseudo-first-order rate constants for disappearance of **1** and

Scheme I

$$1 + HO_2^- \overset{K_1}{\rightleftharpoons} 1(OOH) \underset{k_{-2}[H_3O^+]\ k_{-3}[H_2O]}{\overset{k_2[H_2O]\ k_3[HO^-]}{\rightleftharpoons}} 1(OO^-) \xrightarrow{k_6} 2 + 2^*$$

$$1(OOH) \underset{k_{-4}[H_3O^+]\ k_{-5}[H_2O]}{\overset{k_4[H_2O]\ k_5[HO^-]}{\rightleftharpoons}} 1(OOH)OH \xrightarrow{k_7} 2 + 2$$

CL decay increase linearly with $[H_2O_2]_T$ (inset Figure 3a). This information when taken with the fact that Φ_{CL} remains constant over the measured range of $[H_2O_2]_T$ at various pHs (Table V) establishes that both CL and non-CL reactions are first order in $[H_2O_2]_T$ at all examined pH values. (If only the CL reaction possessed a first-order dependence upon $[H_2O_2]_T$, Φ_{CL} would increase with the first power of $[H_2O_2]$. If only the non-CL reaction possessed a first-order dependence upon $[H_2O_2]$, Φ_{CL} would decrease with the first power of $[H_2O_2]$.)

The fact that rates of both disappearance of **1** (k_{obsd}) and light emission decay (k_b) vary in an equivalent manner with change of pH (Figure 3a) while Φ_{CL} is pH invariant (Table VI) shows that both reactions possess the same dependence upon $[HO^-]$. (If the CL and non-CL reactions did not have the same dependence upon $[HO^-]$, then Φ_{CL} would not be invariant with pH.)

Finally, the stoichiometry of the emitter (**2***) relative to starting material (**1**) was determined to be 1:1 by the fact that rates of both CL and non-CL reactions are first order in **1** (Table VII) and that total quanta emitted have a first-order dependence upon [**1**] (Figure 4). These data indicate that the CL and non-CL paths for conversion of **1** into **2** are kinetically identical.

Since no buffer effect is seen in the pH range examined (Table III), the pH-dependent behavior of k_{obsd} and k_b reflects either specific base catalysis and/or the involvement of HO^- as an essential nucleophilic component. The log (rate constant) vs. pH profile of Figure 3a allows a number of conclusions to be drawn. First, the change in slope of the profile from one to zero with increasing pH is in accord with the formation of a pseudobase by HOO^- or HO^- addition to **1**. That the pH-log k_{rate} profile inflects at approximately the pK_a of H_2O_2 is evidence for the addition of HO_2^- to **1**. At higher pH values both k_{obsd} and k_b become dependent upon $[HO^-]$. This requires that hydroxide addition or kinetically equivalent proton abstraction is involved subsequent to addition of HO_2^- to **1**. Any postulated mechanism must therefore take into account equilibrium addition of HO_2^- to lucigenin with subsequent spontaneous and HO^--catalyzed pathways for adduct decomposition. Assuming that the low values of Φ_{CL} result from competing CL and non-CL reactions, with the latter predominant, the simplest mechanistic sequence which provides kinetically identical CL and non-CL paths is that of Scheme I. The sequence of reactions involving the terms K_1, k_4 and K_1, k_2 represents the portions of the log k_b and log k_{obsd} vs. pH profile (Figure 3a) of slope +1 to zero while the sequence K_1, k_3 $[HO^-]$ and K_1, $k_5[HO^-]$ represents that portion of the profiles at high pH where the slope again increases to +1. The CL reaction may be accounted for through the formation of a dioxetane (Scheme II). The kinetically identical non- or very weakly chemiluminescent reaction may then be accounted for by the acyclic peroxide decomposition mechanism of Scheme III. (The essentially non-CL nature of the linear peroxide decomposition of Scheme III is suggested by analogy to the non-CL decomposition of the *tert*-butyl hydroperoxy adduct of **1**; see below.) For Scheme I, at low to moderately basic conditions the rate-determining steps are associated with

Scheme II

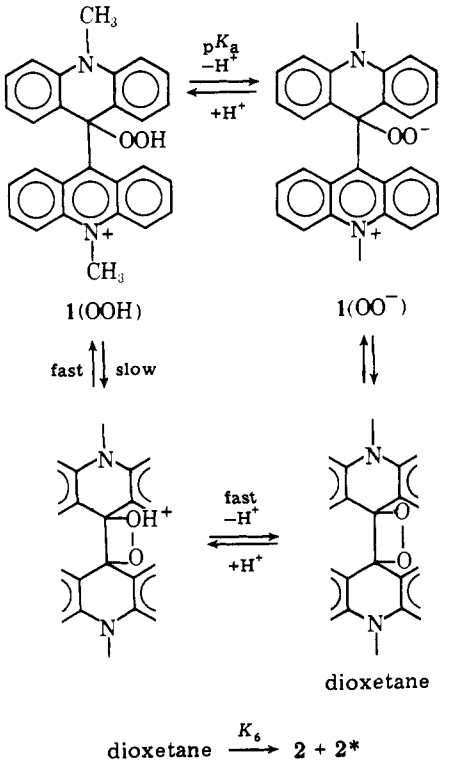

$k_2[H_2O]$ and $k_4[H_2O]$ while at higher pH values $k_3[HO^-] > k_2[H_2O]$ and $k_5[HO^-] > k_4[H_2O]$. The equilibrium associated with K_1 must be established rapidly since there is no buildup of the precursor to the excited species (i.e., plots of cps vs. time do not show a sequential first-order appearance and disappearance of counts with time). That the mechanisms of Scheme I are kinetically competent may be shown by either steady-state assumptions in **1**(OO$^-$) and **1**(OO)OH or by material balance in **1**(OOH), **1**(OO$^-$), **1**(OOH)OH, and **1**. The steady-state assumption provides eq 4, which is mathematically identical with the experimentally obtained rate law of eq 1.

$$k_{obsd} = \frac{K_1 K_a}{K_a + a_H}\left\{(k_4 k_2) + \frac{K_w}{a_H}\left[\frac{k_6 k_3}{k_6 + k_{-3}} + \frac{k_7 k_5}{k_7 + k_{-5}}\right]\right\}[H_2O_2]_T \quad (4)$$

A number of alternate mechanisms[12-14] have been proposed for the reaction of **1** with basic hydrogen peroxide. However, most of these can be ruled out since they do not lead to formation of *N*-methylacridone as the excited species. The competition between dioxetane and linear peroxide mechanisms (as in Schemes II and III) has been observed in several CL reactions.[15,16] In the case of α-hydroperoxy ketones, Sawaki and Ogata[16a] have shown the linear mechanism to be predominant, depending upon the structure of the hydroperoxide. McCapra[12] has speculated on the possibility of both the cyclic and acyclic mechanisms for reaction of hydrogen peroxide with **1** but was unable to distinguish between the two owing to lack of conclusive evidence. The reaction of $^1O_2$ with 10,10′-dimethyl-9,9′-biacridylidene (**5**) to provide a strong CL by **2*** has reasonably been interpreted to involve the intermediacy of the dioxetane of Scheme II (as in eq 5).[17]

Scheme III

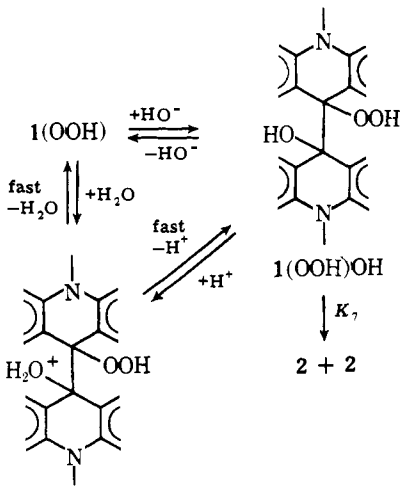

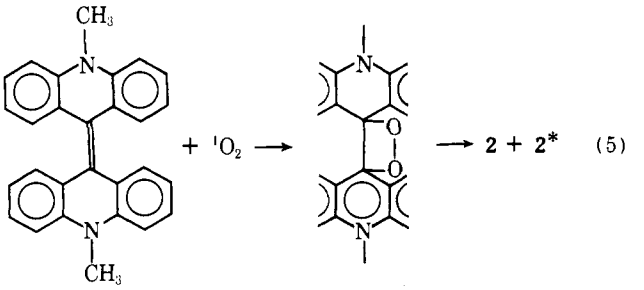

A means of judging the plausibility of Schemes II and III is available through the substitution of H_2O_2 by an alkyl peroxide (as *t*-BuOOH). An alkyl peroxide adduct of **1** would be expected to enter into the elimination reaction of Scheme III but could not form a dioxetane as in Scheme II. Comparison of pH vs. rate constant profiles for the reaction of hydrogen peroxide and *tert*-butyl hydroperoxide (at 0.035 M) with **1** (Figure 3b) shows the reaction with *t*-BuOOH to be an order of magnitude slower than the reaction with H_2O_2, but several orders of magnitude faster than the disappearance of **1** from solution in the absence of a peroxide (i.e., aerobic reaction at alkaline pH).[8] Comparison of Figure 5 with Table VI shows Φ_{CL} for the *t*-BuOOH reaction to be two orders of magnitude lower than Φ_{CL} for the reaction of hydrogen peroxide with **1**. In the *t*-BuOOH reaction the quanta emission increases and then decreases following the kinetic equations for consecutive first-order processes. This is a characteristic of the CL reaction of **1** at basic pH values in the presence of O_2.[8] The quanta emission in the hydrogen peroxide reaction follows a simple exponential decay. The pH dependence of Φ_{CL} in the *t*-BuOOH reactions follows the same pH dependence as does the CL reaction of **1** in aerobic basic solutions, i.e., is independent of pH. However, Φ_{CL} for the *t*-BuOOH reaction is actually somewhat smaller (Figure 5). Purification of *t*-BuOOH by recrystallization of its sodium salt results in a drop in the observed value of Φ_{CL} during the first three recrystallizations. Further recrystallization (six times) does not result in a further decrease in Φ_{CL}. An increase in [*t*-BuOOH] at constant pH actually results in a decrease in Φ_{CL}. Though the reaction of *t*-BuOOH with **1** may show some CL, it must be concluded that light production is minimally several powers of ten less than that seen with hydrogen peroxide and indeed less than that observed in weakly basic solutions in the absence of any added peroxide. The chemiluminescence observed in the presence of *t*-BuOOH may be explained as being due to the aerobic oxidation of **1** at high pHs which is depressed owing to siphoning off of **1** by its reaction with *t*-BuOOH. Our suggestion that *t*-BuOOH reacts with **1** through the linear peroxide mechanism of Scheme II appears reasonable. The only fluorescent species present in the spent reaction solutions from the reaction of **1** in the presence of *t*-BuOOH is **2**. The linear mechanism therefore appears to have a very low efficiency in the production of **2***.

Hydrogen peroxide ion is considered as a reductant of **1** in

Scheme IV

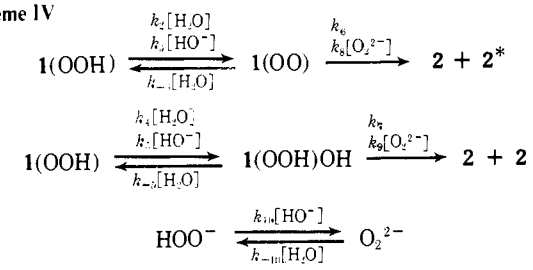

Scheme V

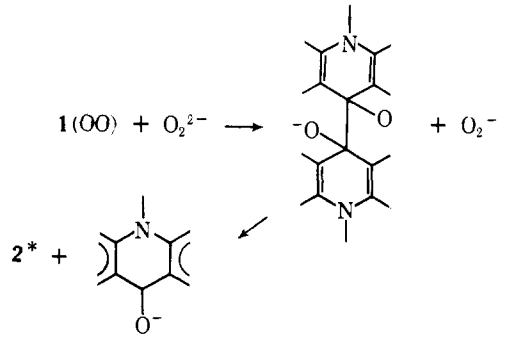

a mechanism proposed by Totter.[13] Though $1e^-$ transfer from HO_2^- is thermodynamically favored at pH values much above 10, the end result is likely to be indistinguishable from the nucleophilic addition of HO_2^- to **1**:

$$\mathbf{1} + HO_2^- \text{—}[\mathbf{1}\cdot + HO_2\cdot]\rightarrow \mathbf{1}(OOH) \qquad (6)$$

It is our feeling that the production of reduced **1** does not lead to a CL reaction per se. Thus, we find that the half-wave oxidation potential of HO_2^- (−0.115 vs. SCE, 30°C, μ = 1 with KCl, pH 11.95) is less negative (i.e., is a poorer reducing agent) than the potential of t-BuO_2^- (−0.365 vs. SCE) which is ineffective in terms of light production in its reaction with **1**.

What has been presented in the Discussion up to this point is a description of kinetically competent mechanisms based on multiple data. What follows is a kinetically allowed (but speculative) proposal to account for the observation that the rate of light emission (k_b) exceeds to an extent the rate (k_{obsd}) of disappearance of starting material (**1**) at high pH values.

The data presented in Figure 3a shows that k_b:k_{obsd} varies from ~1:1 at lower pHs to ratios of >2:1 at higher pH values. The experiments providing the pH-rate constant profiles were repeated on several occasions with different sources of H_2O_2 and fresh solutions of **1**. In each instance $k_b > k_{obsd}$ at high pHs (in one instance increasing from a ratio of 1:1 to 5:1). An explanation for this finding is not evident in the reaction sequence of Scheme I unless additional mechanisms are added for the cyclic decomposition of **1**(OO) (Scheme II) and the acyclic decomposition of **1**(OOH)OH (Scheme III) at high pH. Scheme IV provides an additional set of reaction steps which may explain this divergence.

If one assumes that at low pH all intermediates [**1**(OOH), **1**(OO), **1**(OOH)OH, and **1**(OH)] are in equilibrium then the kinetics are controlled by the major reaction path (through k_7) and $k_b = k_{obsd}$. An increase in pH must then uncouple the equilibrium so that **1**(OO) and **1**(OOH)OH, once formed, go on to product without being reconverted to **1**(OOH). If this were so, k_b need not equal k_{obsd}. If the intermediate leading to **2*** (i.e., **1**(OO)) decomposes more rapidly at high pH than does the intermediate into which most of **1** has been converted (i.e., **1**(OOH)OH), then a net divergence in k_b and k_{obsd} will occur with $k_b > k_{obsd}$. For Scheme IV, one must then assume that $k_{-3} > k_6$ and $k_{-5} > k_7$ (system is in equilibrium), and

Scheme VI

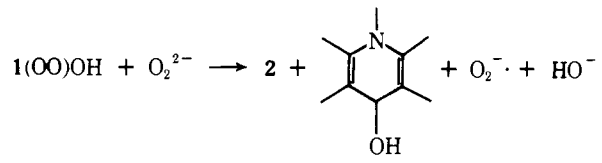

$k_8[O_2^{2-}]$ and $k_9[O_2^{2-}]$ are unimportant at low pH and become important at high pH when $k_8[O_2^{2-}] > k_{-3}$ and $k_9[O_2^{2-}] > k_{-5}$ (system is uncoupled). The kinetic competence of Scheme IV was tested employing an iterative reaction kinetics simulator and found to be competent: (a) disappearance of **1** [and intermediates **1**(OOH), **1**(OOH)OH, and **1**(OO)] follow the first-order rate law at all pH values; (b) appearance of **2*** follows the first-order rate law at all pH values; (c) the quantum yield is pH insensitive; (d) the forms of the log k_{rates} vs. pH profiles are as in Figure 3a, i.e., the rate constants generated by the simulation show the same dependence on pH as do the experimental data; (e) the ratios of k_b:k_{obsd} increase with increasing pH; (f) k_b is independent of the initial [**1**]. The catalytic sequences representing the reaction paths associated with $k_8[O_2^{2-}][\mathbf{1}(OO)]$ and $k_9[O_2^{2-}]\cdot[\mathbf{1}(OOH)OH]$ may then be as depicted in Schemes V and VI.

The mechanism of Scheme V is an example[18] of chemiluminescence brought about by $1e^-$ transfer to a cyclic peroxide. A surprising aspect of the CL pathway presented in Scheme V is the apparently small difference between the efficiency of producing excited states (Φ_{Ex}) in the spontaneous dioxetane decomposition pathway (Scheme II) and the electron-initiated dioxetane decomposition pathway (Scheme V). Substantial differences between Φ_{Ex} for the two pathways would have resulted in a change in Φ_{CL} at high pHs, where Scheme V would be predominant (see Table VI).

Acknowledgment. We would like to thank Dr. Cemal Kemal for his helpful suggestions during the course of this research. This work was supported by a grant from the National Science Foundation.

References and Notes

(1) B. Radziszewski, *Ber.*, **10**, 70, 321 (1877).
(2) H. O. Albrecht, *Z. Phys. Chem. (Leipzig)*, **136**, 321 (1928).
(3) K. Gleu and W. Petsch, *Angew. Chem.*, **48**, 57 (1935).
(4) A. A. Frost and R. G. Pearson, "Kinetics and Mechanisms," Wiley, New York, 1953, Chapter 8.
(5) (a) H. Decker and W. Petsch, *J. Prakt. Chem.*, **143**, 211 (1935); (b) K. Gleu and A. Schubert, *Ber.*, **73**, 757 (1940).
(6) J. R. Hlubucek, E. Ritchie, and W. C. Taylor, *Aust. J. Chem.*, **23**, 1881 (1970).
(7) E. L. O'Brian, F. M. Beringer, and R. B. Mesrobian, *J. Am. Chem. Soc.*, **79**, 6238 (1957).
(8) R. Maskiewicz, D. Sogah, and T. C. Bruice, *J. Am. Chem. Soc.*, following paper in this issue.
(9) H. S. Harned and K. A. Robinson, *Trans. Faraday Soc.*, **36**, 973 (1940).
(10) R. D. Mair and J. A. J. Granpher, *Anal. Chem.*, **36**, 144 (1964).
(11) A. J. Everett and G. J. Minkoff, *Trans. Faraday Soc.*, **49**, 410 (1953).
(12) F. McCapra in "Acridines", R. M. Acheson, Ed., Wiley, New York, 1973, pp 615-630; F. McCapra, *Prog. Org. Chem.*, **8**, 231 (1973).
(13) (a) J. R. Totter, *Photochem. Photobiol.*, **3**, 231 (1964); (b) J. R. Totter and G. E. Philbrook, *ibid.*, **5**, 177 (1966); (c) J. R. Totter, *ibid.*, **22**, 293 (1975).
(14) A. M. Grigorovsky and A. A. Simenov, *J. Gen. Chem. USSR (Engl. Transl.)*, **21**, 653 (1951).
(15) (a) W. H. Richardson, V. F. Hodge, D. L. Stiggall, M. B. Yelvington, and F. C. Montgomery, *J. Am. Chem. Soc.*, **96**, 6652 (1974); (b) W. H. Richardson and V. F. Hodge, *ibid.*, **93**, 3996 (1971).
(16) (a) Y. Sawaki and Y. Ogata, *J. Am. Chem. Soc.*, **99**, 5412 (1977); (b) Y. Sawaki and Y. Ogata, *ibid.*, **97**, 6983 (1975).
(17) W.-W. Lee and L. A. Singer, *J. Org. Chem.*, **41**, 2685 (1976).
(18) (a) J. Koo and G. B. Schuster, *J. Am. Chem. Soc.*, **99**, 6107 (1977); (b) *ibid.*, **100**, 4496 (1978); (c) F. McCapra, *J. Chem. Soc., Chem. Commun.*, 946 (1977); (d) K. A. Zaklika, A. L. Thayer, and A. P. Schaap, *J. Am. Chem. Soc.*, **100**, 4916 (1978).